Incorporating Texture Intensity Information into LBP-Based Operators

M. Ghahramani, Guoying Zhao, and Matti Pietikäinen

Center for Machine Vision Research
Department of Computer Science and Engineering
University of Oulu, Finland
{mghahram,gyzhao,mkp}@ee.oulu.fi

Abstract. In this paper, we aim to improve the accuracy of LBP-based operators by including texture image intensity characteristics in the operator. We utilize shifted step function to minimize the quantization error of the step function to obtain more discriminative operators. Features obtained from shifted step function are simply fused together to form the final histogram. This model is generalized and can be integrated with other existing LBP variants to reduce quantization error of the step function for texture classification. The proposed method is integrated with multiple LBP-based feature descriptors and evaluated on publicly available texture databases (Outex_TC_00012 and KTH-TIPS2b) for texture classification. Experimental results demonstrate that it not only improves the performance of operators it is integrated with but also achieves higher accuracy compared to the state of the art in texture classification.

Keywords: Texture, LBP, Intensity information.

1 Introduction

Algorithms proposed for texture classification [1], [2] have been applied to many computer vision applications such as object recognition, remote sensing, and even for recognizing people using biometric modalities [3]. In general texture is defined without restriction on orientation, scale or direction. Rotation invariant features are proposed to classify textures [4], [5]. However, performing texture classification robust to image photometric changes is still an open problem.

Histograms of local descriptors computed from the image can be successfully applied for texture analysis [4]. Local Binary Patterns, LBP describe the image by the sign of subtracting the centre pixel from surrounding pixels. It is shown to be computationally light and invariant to monotonic intensity changes. Some researchers attempted to enhance the LBP in terms of rotation invariant histogram bin selection, multi-resolution feature extraction and image information enrichment. Ojala et al. investigated which bins are robust to rotation that led to rotation invariant patterns [4]. Mäenpää and Pietikäinen studied the effect of various kernels and neighbourhood pixel selection to compute LBP features for texture analysis [6].

J.-K. Kämäräinen and M. Koskela (Eds.): SCIA 2013, LNCS 7944, pp. 66–75, 2013.

Another direction of improving LBP distinctiveness that has recently attracted researchers is to include the image intensity information in the LBP operator. Image intensity information is embedded either by features characterizing gray-scale information or directly utilizing its value with the LBP operator.

Among feature operators that were intended to enrich the information extracted by LBP, Guo et al. proposed LBP Variance (LBPV) to embed the local gray-scale variance information into the LBP histogram [7]. Another solution was to Complete the LBP (CLBP) by combining the sign, magnitude and central pixel intensity information. [8]. However, the need for image illumination normalization is one of the major drawbacks of using centre pixel gray level in CLBP [9]. In another research work, Ghahramani et al. benefited from the intensity level information of facial images by employing multiple thresholds in the LBP operator to include the missing information of the centre pixel that improved face and family verification performance [10].

The LBP operator calculates the local difference of the centre pixel and its surrounding pixels independently from the centre pixel gray-scale information. Figure 1 presents three samples of texture classes on which corresponding classes are indicated. Using the conventional LBP descriptor the inter-class histogram χ^2 distance of samples in Figure 1 (b) and (c) is '0.0002'. It is apparent the relative intensity levels of centre pixels and their neighbours are different in the two provided texture samples. If centre pixel intensity level information is considered to calculate the histogram (when the step function is shifted by 20); the histogram distance increases significantly by '73' times. Note that the intra-class χ^2 histogram distance between samples in Figure 1 (a) and (b) only increases by '1.7' times, if the step function shifted by 20 is used for LBP descriptor.

In this paper we propose to reduce the step function quantization error in LBP operator to include the relative intensity information in LBP-based operators for texture classification. Unlike [8] and [10], The proposed approach is generally applicable to various LBP modifications. We study the effect of shifting the step function over the pixel intensity range. On selected texture databases we achieve highest accuracy using the same number of neighbouring points 'P' and in the neighbourhood of Radius 'R'. It obtains higher accuracy than the previous operators attempting to include the image intensity level in the LBP such as [8], [9], [10] and [11] and other state-of-the-art operators.

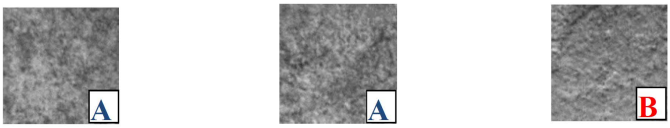

(a) (b) (c)

Fig. 1. Samples from Outex_TC_00012 (a) Class A; (b) Class A; (c) Class B

The rest of the paper is organized as follows, we review LBP based operators in Section 2. In Section 3, we propose our solution to reduce the quantization error of the LBP sign function. Experiments are conducted on well-known texture databases to verify the accuracy improvement achieved by the proposed approach compared to the state-of-the-art operators for texture classification in Section 4. Finally, Section 5 concludes the paper.

2 A Review on LBP

The LBP operator encodes the gray-scale information of each image pixel and its neighbour as a binary string [4]. Histogram of calculated binary codes represents the LBP feature of the image that characterizes the texture pattern. The LBP feature is calculated for centre pixel 'g_c' where it is surrounded by pixel 'g_p' as in equation (1),

$$\mathrm{LBP}_{P,R}(c) = \sum_{p=0}^{P-1} s(g_p - g_c)2^p, \tag{1}$$

where 's' is the sign function,

$$s(x) = \begin{cases} 1, \text{if } x \geq 0; \\ 0, \text{otherwise.} \end{cases} \tag{2}$$

Due to the changes of binary code in case of image rotation, rotation invariant patterns were introduced by Ojala et al. [4]. To benefit from training data, a learning framework was proposed by Guo et al. to obtain discriminative patterns among LBP patterns [11]. It was then formulated into a three-layered model to estimate the optimal pattern subset of interest in terms of robustness, discrimination power and feature representation capability [11]. It was claimed that it can be integrated with existing LBP variants such as the conventional LBP rotation invariant patterns, CLBP and Local Ternary Pattern (LTP) [12] to obtain disLBP^{ri}, dis(S+M)^{ri} and disLTP^{ri} respectively [11]. In order to incorporate contrast of local image texture Ojala et al. proposed to measure the local variance invariant to rotation as,

$$\mathrm{VAR}_{P,R}(c) = \frac{1}{P}\sum_{p=0}^{P-1}(g_p - \mu), \quad where \quad \mu = \frac{1}{P}\sum_{p=0}^{P-1} g_p \tag{3}$$

They stated that it is invariant against shifts in gray-scale by definition. The feature was named VAR. Since LBP^{riu2} and VAR are complementary operators, they defined joint distribution of LBP^{riu2} and VAR as LBP/VAR, a precise and rotation invariant measure of local image texture [4]. It was shown to be robust in terms of gray-scale variations based on the obtained experimental results. The training was performed on a particular rotation angle and tested with samples from other rotation angles.

Recently, LBP Histogram Fourier transform (LBP-HF) proposed by Zhao et al. provided high accuracy in static and dynamic texture recognition [9]. It is

computed from discrete Fourier transforms of LBP histograms. It can be easily generalized to apply to other uniform operators. They proved it is more robust against image rotation and photometric changes and achieved higher accuracy than original domain histograms [9]. For example, LBP-HF, LBPHF_M and LBPHF_S_M can be developed by computing the discrete Fourier transforms of LBP, LBP_M and LBP_S_M, respectively. On the other hand, Texton-based representations were also proposed for texture classification [13].

The one-level sign function employed in the LBP maximizes the quantization error. This drawback exists in other approaches using the step function in the literature as the output does not make any difference for all positive values or on the other side for all negative values. Next, we illustrate our proposed method to reduce quantization error of step function used in LBP-based operators by increasing quantization level and fully incorporate image intensity pattern.

3 The Proposed Solution

Our purpose is to reduce quantization error of the sign function utilized in LBP-based operators. As illustrated earlier, three samples of texture classes from Outex_TC_00012 [14] are depicted in Figure 1. Corresponding classes are indicated on image samples. In fact, Class A contains pixels that their neighbours' gray-values change significantly relative to the centre pixel compared to that of Class B. Using the conventional LBP descriptor the inter-class histogram χ^2 distance of samples in Figure 1 (b) and (c) is '0.0002'. If we use a shifted step function for LBP operator to consider the relative intensity difference between centre pixel and its neighbour the histogram distance becomes '0.0146'. Their χ^2 distance increases by '73' times to '0.0002' while their average intra-class χ^2 distance is approximately equal for class A.

Henceforth, we aim to incorporate the missing information of texture's local relative gray-scale characteristics into the LBP operator. We propose to reduce the quantization error of the step function generally used in the LBP operator. As our goal is to incorporate the local relative intensity changes the resulting operator will not affect illumination robustness of the operator.

Our solution involves selecting thresholds to shift the step function over the possible gray-scale changes. Since intensity changes from pixel to pixel vary [-P_d, P_d], it should span this range of Pixel depth 'P_d'. In general, quantization levels could be Uniformly or Non-uniformly adjusted. We select Uniformly-sampled Thresholds for the step function utilized in the LBP-based operators. Assume that a General LBP-based operator denoted by GLBP is a function of s(x) in equation (2) denoted by $J(s(g_p - g_c))$,

$$\mathrm{GLBP}_{P,R}(c) = J(s(g_p - g_c)), \tag{4}$$

We propose to use 'K' thresholds uniformly sampled in the range of [-P_d, P_d] to shift the step function. The resulting Uniformly-sampled Thresholds for GLBP operator denoted by UTGLBP is the union of features evaluated with different thresholds as,

$$\text{UTGLBP}_{P,R}(c) = \cup_{i=1}^{K} utglbp_{P,R}(c, Thr_i), \tag{5}$$

where,

$$\text{utglbp}_{P,R}(c, Thr_i) = J(s(g_p - g_c - Thr_i)) \tag{6}$$

This opens the problem how to adjust thresholds sampling steps, denoted by 'Thr_i', select distinctive thresholds among sampled thresholds and fuse features evaluated using each threshold. Our answer to these questions is to select 'Thr_i' and concatenate features evaluated from thresholds to create one vector. In cases that testing set does not contain major unseen samples, distinctive thresholds could be selected for each class to reduce feature dimension while maintaining the accuracy. We choose to simply select threshold indices for feature concatenation for odd number of thresholds. We assume that '$Thr = 0$' is among thresholds and its index is '(K+1)/2' where 'K' is odd. If total number of feature sets extracted from thresholds to be concatenated is equal to 'K=2n+1' the UTGLBP is evaluated as,

$$\text{UTGLBP}_{P,R}(c) = \cup_{j=-n}^{n} utglbp_{P,R}(c, Thr_{j+\frac{K+1}{2}}) \tag{7}$$

Feature Dimension Reduction

The proposed descriptor can be easily applied to LBP-based operators and improves their accuracy in texture classification. LBP-HF produces 38, 138 and 302 features for 'P' equal to 8, 16 and 24 respectively compared to LBP^{riu2} producing 10, 18 and 26 for the same settingsi. We suggested concatenating 'n' thresholds from 'K' uniformly sampled thresholds and it increases feature dimension by 'n' times. Hence UTLBP-HF(24,3) produces very sparse feature vector of size (n*302). To tackle this problem, we propose a simple hypothesis to check among all histograms generated from 'K' thresholds which bins differ among classes. We perform a simple inter-class histogram difference calculation among the training set and calculate their summation. The calculated histogram is then normalized and the bins that are smaller than 10^{-4} are removed from the overall concatenated histogram of all 'K' histograms. The performance achieved after feature dimension reduction of UTLBP-HF is reported in parenthesis '()' in Tables 2 and 3.

4 Experiments and Discussion

We evaluate the performance of various well-known high performance LBP-based operators with/without integrating the proposed shifted step function and comparisons are made among them. Experiments are conducted on two texture databases: Outex_TC_00012 [14] and the challenging KTH-TIPS2b database [15] for material classification. In the first set of experiments conducted on Outex_TC_00012, we evaluate the performance of LBP [4], LBP-HF [11] with our proposed multi-step function integrated with them. Results of multiple subsets of histogram bins that are shown to be robust against rotation 'ri' [4] and '$riu2$'

[4] are also included. In addition, other operators aiming to tackle the lack of relative gray-scale difference information in the LBP step are examined. As the first step, operators listed in Table 1 were all tested on Outex_TC_00012 to examine which could obtain the highest accuracy while trying to benefit from pixel intensity information.

In the second part of experiments we validate the performance obtained by the most discriminative operator with Uniformly-sampled Thresholds for feature operators on the Outex database on a more challenging texture database to validate our results. We choose the material classification database that contains samples of multiple classes of substances captured under illumination, pose and scale changes known as KTH-TIPS2b the material database [15].

To have fair comparisons of operators performances which depend on their distinctiveness, we adapt the same experimental settings as explained in [4]. Features of training samples are extracted and the non-weighted χ^2 distance is utilized to measure the dissimilarity between histograms. Based on standard protocols the nearest neighbour classifier (1-NN) decides which class in the training set the query sample belongs to [14], [15].

Do note that, no illumination normalization is utilized to be fair to other operators. In all experiments thresholds are selected for P_d=256 and Thr_i=10. we consider thresholds from -100 to 100 as large pixel differences are quite rare to happen in neighbourhood pixels. It generates 'K=21' thresholds where features evaluated at 11^{th} shifted step function are equivalent to the original step function and 'n=10'. We choose number of thresholds to be concatenated when adding further shifted step functions does not improve the accuracy significantly.

4.1 Experiments on the Outex_TC_00012

Outex_TC_00012 contains 24 texture classes. Using the 'inca' illuminant, 20 samples were captured from each class and the training is done on 480 samples as described in [14]. The test set comprises samples collected under two separate scenarios. Problem '000' contains rotated samples captured under the 'tl84' illuminant and Problem '001' comprises samples illuminated by '*horizon*'. Each problem consists of 4320 samples that results in 8640 samples. We report our results as the mean accuracy obtained in both problems '000' and '001'.

Using the feature operator abbreviations indicated in Table 1, we compare accuracies of LBP_M^{u2} [8], LBP_M^{riu2} [8], LBPHF_M [9], $LBP\_S\_M^{riu2}$ [8], LBPHF_S_M [9], VAR [4] and LBP/VAR [4] on the Outex_TC_00012 database. These results were adopted from [9] and we used the LBP MATLAB implementation from www.cse.oulu.fi/CMV/Downloads/LBPMatlab. We analyse the accuracy improvement achieved by integrating the proposed step function by comparing the accuracy of LBP^{riu2} [4], LBP-HF [9] with $UTLBP^{riu2}$ and UTLBP-HF respectively.

Moreover, Guo et al. [11] proposed $disLBP^{ri}$, $dis(S+M)^{ri}$ and $disLTP^{ri}$ features to select discriminative features of LBP, CLBP [8] and LTP [12] respectively and we quote their results for further comparison. Note that performance of LBP_M^{u2}, LBP_M^{riu2}, LBPHF_M, $LBP\_S\_M^{riu2}$, LBPHF_S_M and

Table 1. Notations and their corresponding definitions in this paper

Abbreviation	Method
LBP^{u2}	Uniform sign LBP
LBP^{riu2}	Rotation invariant uniform sign LBP
LBP_M^{u2}	Uniform magnitude LBP
LBP_M^{riu2}	Rotation invariant uniform magnitude LBP
$LBP\_S\_M^{riu2}$	Concatenation of sign LBP^{riu2} and magnitude LBP^{riu2}
LBP-HF	Uniform LBP histogram Fourier
LBPHF_M	Uniform magnitude LBP histogram Fourier
LBPHF_S_M	Concatenation of sign & magnitude LBP histogram Fourier
$disLBP^{ri}$	The Discriminative Local Binary Patterns
$dis(S+M)^{ri}$	The Discriminative Completed LBP
$disLTP^{ri}$	The Discriminative Local Ternary Pattern
VAR	Rotation Invariant Variance measure of the image contrast
LBP/VAR	Joint distribution of LBP^{riu2} and VAR
VZ-MR8	VZ algorithm obtained from (MR8) filters
VZ-Joint	VZ algorithm obtained from original image patches
UTLBP	Uniformly-sampled Thresholds for LBP
UTLBP-HF	Uniformly-sampled Thresholds for LBP-HF

VAR, LBP/VAR and $disLBP^{ri}$, $dis(S+M)^{ri}$, $disLTP^{ri}$ are quoted from [9], [4] and [11] respectively. We also compare texton-based representation to model the Markov Random Fields (MRF) joint neighbourhood distribution in [5]. The early version of Varma-Zisserman (VZ) algorithm uses the Maximum Response 8 (MR8) filters with various pixel window sizes support, known as VZ-MR8 [5]. The second version was then modified in the way that the source image patches are directly utilized in the joint representation [13].

Texture classification accuracies are shown in Table 2 for all aforementioned operators listed in Table 1 on this database using threshold concatenation. We observe that improvements are achieved in several aspects:

1. Various feature operators aim to tackle the lack of relative pixel intensity information in LBP-based operators, such as LBPHF_M [9], $LBP\_S\_M^{riu2}$ [8], $LBPHF\_S\_M$ [9], VAR [4] and LBP/VAR [4]. Our proposed step function can successfully embed the missing information in the operators LBP and LBP-HF to obtain more discriminative operators UTLBP and UTLBP-HF respectively. The improvements achieved by UTLBP and UTLBP-HF relative to LBP and LBP-HF are comparable to other LBP enhancements independent from neighbour settings.
2. Unlike descriptors such as VAR for which the accuracy reduces when radius increases from 2 to 3, increasing the radius improves the accuracy on proposed UTLBP-HF.
3. UTLBP-HF outperforms selected state-of-the-art descriptors. The proposed feature dimension reduction method in Section 3 reduces UTLBP-HF dimension to 6 and 4 times of LBP-HF for 'P' equal to 16 and 24 respectively and their performance is reported in parenthesis in Table 2.

We test the most discriminative feature operators from the Outex_TC_00012 i.e. UTLBP and UTLBP-HF, on a more demanding database to validate their discrimination power with the well-known state-of-the-art operators.

Table 2. Performance of the state-of-the-art operators and the proposed method with different (P,R) parameters on the Outex_TC_00012. Accuracies in parenthesis are with feature dimension reduction in Section 3.

Database	Method	(8,1)	(16,2)	(24,3)
Outex TC 00012	LBP^{u2}	56.9	58.9	56.9
	LBP^{riu2}	64.6	78.9	83
	$UTLBP^{riu2}$	81.1	92.3	93.6
	LBP-HF	74.1	90.3	92.4
	UTLBP-HF	**85.9**	**97 (96.5)**	**97.7 (97.8)**
	LBP_M^{u2}	49.6	56.7	59.4
	LBP_M^{riu2}	61	73.1	79.9
	LBPHF_M	62.2	85.6	87.4
	LBP_S_M^{riu2}	71.4	86	90.4
	LBPHF_S_M	78.6	94	94.9
	VAR	64.5	69.5	65.8
	LBP/VAR	77.8	85.4	86.9
	disLBP^{ri}	68.3	84.5	91.6
	dis(S +M)^{ri}	74.1	92.9	95.9
	disLTP^{ri}	69	89.1	95

4.2 Experiments on KTH-TIPS2b

The challenging KTH material database contains Textures under Illumination, Pose and Scale variations known as KTH-TIPS2b. It consists of 11 materials each with 4 different subcategories of physical characteristics [15]. We choose the standard protocol as in [15]. We first train on 'b' number of subcategories ($1 \leq b \leq 3$) for all materials and then test on the remaining '4-b' subcategories.

This is repeated for all possible permutations of sets and the average of texture classification accuracy is reported. In this paper, only experimental results for test 3 (b=3) are tabulated due to lack of space. For our proposed method, we select thresholds as the same settings reported for Outex_TC_00012. To prevent from over fitting on training dataset, we report results of concatenating nine thresholds (n=4) for all tests. We compare the results of the best features we obtained from the Outex_TC_00012 experiment on the KTH-TIPS2b database in Table 3. The proposed feature dimension reduction method in Section 3 reduces UTLBP-HF dimension to 3 times of LBP-HF for (R,P)=(3,24). The results in

parenthesis report the performance by only reducing UTLBP-HF(24,3) features in Table 3. The feature dimension reduction is only applied to radius 3 for multi-resolution UTLBP-HF.

Table 3. Texture classification accuracies of the state-of-the-art operators and the proposed operators on the KTH-TIPS2b database/tests

Database/Test	Method	Parameters/types	Accuracy
KTH-TIPS2b Test 3	LBP^{riu2}	(24,3)	57.8
	$UTLBP^{riu2}$	(24,3)	61.6
	UTLBP-HF	(24,3)	66.3 (68.9)
	UTLBP-HF	(8,1) + (16,2) + (24,3)	**67.9 (69.6)**
	LBP^{riu2}	(8,1) + (16,2) + (24,3)	60.3
	$UTLBP^{riu2}$	(8,1) + (16,2) + (24,3)	63
	VZ	MR8	55.7
	VZ	Joint	60.7

The state-of-the-art performance is directly quoted for LBP^{riu2} [15], with radii suggested in [15]. Accuracies of VZ-MR8 and VZ-Joint are also tabulated in Table 3 where 40 textons per class are utilized to build the universal dictionary for every texton [15]. The results show that not only utilizing the proposed UTLBP and UTLBP-HF improves the accuracy of LBP and LBPHF respectively, but also the UTLBP-HF outperforms other state-of-the-art operators on the KTH-TIPS2b database experiments.

5 Conclusion

In this paper, we proposed to embed local relative intensity information of texture images to LBP-based operator. Our solution relies on reducing quantization error of the sign function widely used in LBP and its enhanced operators. The proposed method could be easily applied to the features based on LBP operator. We evaluated the proposed method on two texture databases using their respective suggested testing protocols. The results show that the developed UTLBP-HF achieves the highest accuracy among the stateof- the-art operators in the literature. Moreover, integrating the proposed method to selected operators enhances their accuracy more than other modifications such as VAR, LBP/VAR and CLBP proposed in the literature.

Acknowledgment. The financial support of the Academy of Finland and Infotech Oulu is gratefully acknowledged.

References

1. Tuceryan, M., Jain, A.K.: Texture Analysis. In: Chen, C.H., et al. (eds.) Handbook of Pattern Recognition and Computer Vision. World Scientific (1993)
2. Zhang, J., Tan, T.: Brief Review of Invariant Texture Analysis Methods. Pattern Recognition 35, 735–747 (2002)
3. Ahonen, T., Hadid, A., Pietikäinen, M.: Face Description with Local Binary Patterns: Application to Face Recognition. IEEE Transactions on Pattern Analysis and Machine Intelligence 28(12), 2037–2041 (2006)
4. Ojala, T., Pietikäinen, M., Mäenpää, T.: Multiresolution Gray-Scale and Rotation Invariant Texture Classification with Local Binary Patterns. IEEE Transactions on Pattern Analysis and Machine Intelligence 24, 971–987 (2002)
5. Varma, M., Zisserman, A.: A Statistical Approach to Texture Classification from Single Images. International Journal of Computer Vision 62, 61–81 (2005)
6. Mäenpää, T., Pietikäinen, M.: Multi-scale Binary Patterns for Texture Analysis. In: Proceedings of the 13th Scandinavian Conference on Image Analysis, Halmstad, Sweden (2003)
7. Guo, Z., Zhang, L., Zhang, D.: Rotation Invariant Texture Classification Using LBP Variance (LBPV) with Global Matching. Pattern Recognition 43, 706–719 (2010)
8. Guo, Z., Zhang, L., Zhang, D.: A Completed Modeling of Local Binary Pattern Operator for Texture Classification. IEEE Transactions on Image Processing 19, 1657–1663 (2010)
9. Zhao, G., Ahonen, T., Matas, J., Pietikäinen, M.: Rotation-Invariant Image and Video Description With Local Binary Pattern Features. IEEE Trans. on Image Processing 21, 1465–1477 (2012)
10. Ghahramani, M., Yau, W.Y., Teoh, E.K.: Enhancing Local Binary Patterns Distinctiveness for Face Representation. In: 2011 IEEE International Symposium on Multimedia (ISM), pp. 440–445 (2011)
11. Guo, Y., Zhao, G., Pietikäinen, M.: Discriminative Features for Texture Description. Pattern Recognition (2012)
12. Tan, X., Triggs, B.: Enhanced Local Texture Feature Sets for Face Recognition Under Difficult Lighting Conditions. IEEE Transactions on Image Processing 19, 1635–1650 (2010)
13. Varma, M., Zisserman, A.: A Statistical Approach to Material Classification Using Image Patch Exemplars. IEEE Transactions on Pattern Analysis and Machine Intelligence 31, 2032–2047 (2009)
14. Ojala, T., et al.: Outex - New Framework for Empirical Evaluation of Texture Analysis Algorithms. In: Proceedings of the 16th International Conference on Pattern Recognition (ICPR 2002), vol. 1 (2002)
15. Caputo, B., Hayman, E., Mallikarjuna, P.: Class-Specific Material Categorisation. In: Proceedings of the Tenth IEEE International Conference on Computer Vision, vol. 2 (2005)